The research of the spherical space-time ETAS model

Xiong Ziyao　　リスク解析戦略研究センター 特任助教

1. Introduction

The widely used space-time ETAS (epidemic-type aftershock sequence) model was developed by Ogata (1998). This model successfully explains foreshocks and high order aftershocks in earthquake sequences and provides a very effective tool for seismic activity analysis. However, this space-time ETAS model is only suitable for the study within a small space range. When the space range is large, since the earth is a sphere, the simulation results of the model will produce errors. In this study, we reformulate the model from its planar version to a spherical version, to analyze and forecast global seismicity or seismicity in high latitude regions. The new model is verified by applying it to the global CMT catalog. The results show that the new model can simulate the global seismicity variation well. It provides support for better modeling of seismic activities and seismic interactions in global regions. We also calculate the seismicity rates of the seismicity belt along the western Pacific coast to further analyze the characteristics of earthquake sequences.

2. Spherical space-time ETAS model

- Suppose that the earthquake events $\{(t_i, \xi_i, \eta_i, m_i), i = 1, \cdots, N\}$ is known, the conditional intensity for the model is expressed as:

$$\lambda(t, \xi, \eta | \mathcal{H}_t) = \nu\mu(\xi, \eta) + \sum_{i:t_i<t} \kappa(m_i) g(t - t_i) f(\delta(\xi, \eta; \xi_i, \eta_i); m_i)$$

- In this model, $\kappa(m)$, $g(t)$ and $f(\delta; m)$ can be expressed as:

$$\kappa(m) = A\exp[\alpha(m - m_c)], \quad m \geq m_c,$$

$$g(t) = \frac{p-1}{c}\left(1 + \frac{t}{c}\right)^{-p}, \quad t > 0,$$

$$f(\delta; m) = \frac{q-1}{4\pi} \frac{\left(De^{\gamma(m-m_c)}\right)^{-q}}{\left(De^{\gamma(m-m_c)}\right)^{1-q} - \left(1 + De^{\gamma(m-m_c)}\right)^{1-q}} \left(1 + \frac{\text{hav}\,\delta}{De^{\gamma(m-m_c)}}\right)^{-q}$$

with $\text{hav}\,\delta = \sin^2\frac{\delta}{2} = \frac{1-\cos\delta}{2}$ being the haversine function.

- The logarithmic likelihood function of the conditional intensity is expressed as

$$\ln L(\boldsymbol{\theta}) = \sum_{i:(t_i,\xi_i,\eta_i)\in S\times[T_1,T_2]} \ln\lambda\left(t_i, \xi_i, \eta_i \middle| \mathcal{H}_{t_i}\right) - \iint_S \int_{T_1}^{T_2} \lambda(t, \xi, \eta | \mathcal{H}_t) dt d\xi d\eta$$

$$\boldsymbol{\theta} = (\nu, A, \alpha, c, p, D, q, \gamma)$$

- The probability that ith event is a background event is $\varphi_i = \frac{\mu\left(\xi_i, \eta_i \middle| \mathcal{H}_{t_i}\right)}{\lambda\left(t_i, \xi_i, \eta_i \middle| \mathcal{H}_{t_i}\right)}$

- The background seismicity rate can be estimated as

$$\hat{\mu}(\xi, \eta) = \frac{1}{T}\sum_{i=1}^{N} \varphi_i Z(\delta(\xi, \eta; \xi_i, \eta_i); \sigma_i) \ ,$$

in which $Z(\delta; \sigma)$ is: $Z(\delta; \sigma) = \frac{\exp(-\frac{\sin^2\frac{\delta}{2}}{2\sigma^2})}{8\pi\sigma^2\left(1 - e^{-\frac{1}{2\sigma^2}}\right)}$ with $\sigma = De^{\gamma(m-m_c)}$

3. Application

[The boundary representation of the study area]

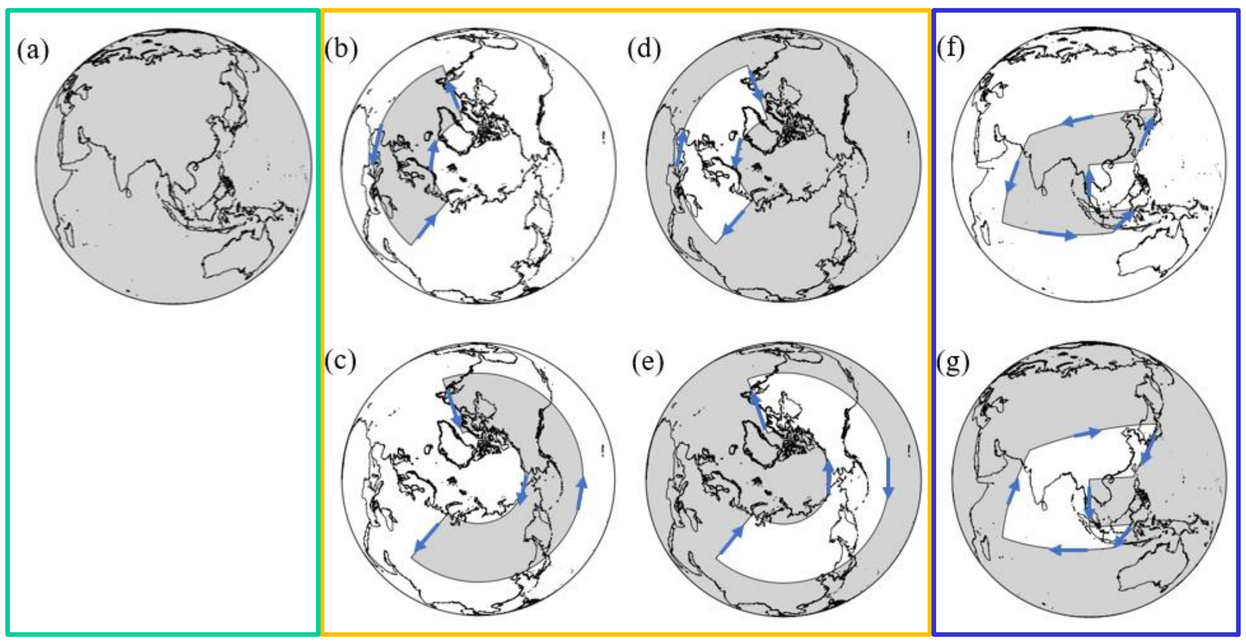

➢ Figure 1. An example of (a) no boundary, (b)/(c)/(d)/(e) quadrilateral boundary, and (f)/(g) spherical polygon boundary. The gray regions represent the study areas, the arrows represent the directions along the boundary. And different regions are determined by the direction of vertices.

[Data]

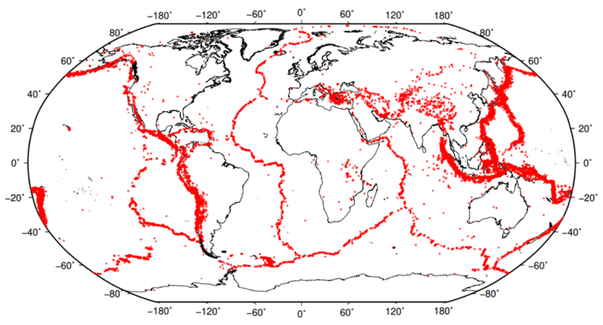

➢ Figure 2. Epicenter locations of global seismicity (Global Centroid-Moment-Tensor (CMT) catalog Mw>=5.15, from January 1, 1996, to October 31, 2021)

[Stochastic reconstruction]

- Based on the method of zhuang et al. (2004), we can obtain the reconstruction result of earthquake epicentral location $\hat{f}(r)$, which can be expressed as:

$$\hat{f}(r) = \frac{\sum_{i,j} \rho_{ij} I(r_{ij} \epsilon [r - \Delta r/2, r + \delta r/2])}{\delta r \sum_{i,j} \rho_{ij}}$$

r_{ij} is the normalized great arc distance (in radian) between two points.

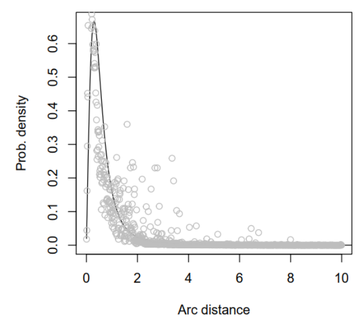

➢ Figure 3. Reconstruction results for the triggering distance $\hat{\boldsymbol{f}}(\boldsymbol{r})$(gray circles). Theoretical curve is plotted by solid line.

[Seismicity Rate estimation and parameter comparation]

- We apply the new model to the global CMT catalog and consider the case of no boundary. The estimated total seismicity rate and background seismicity rate can be seen in Figures 4 and 5. The results show that the new model can simulate the global seismicity variation reasonably. And Table shows the estimation results of model parameters (Area 1).
- Furthermore, we apply the quadrilateral boundary type, and the spherical polygon boundary type to remove an area without earthquakes (the longitude ranges from 160° to -170° and the latitude from 0° to 30°), and the remaining areas are Area 2 and Area 3, respectively. As shown in Table, the calculation results of the three areas are the same, which verifies the accuracy of the algorithms of different boundary types.

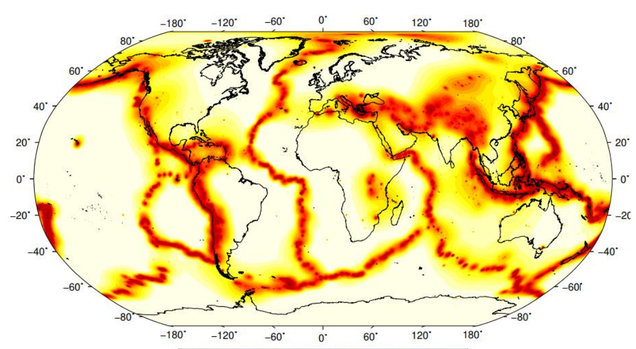

➢ Figure 4. Spatial variation of **total seismicity rates** (event/day/deg^2) for Mw>=5.15 calculated by Spherical spatiotemporal ETAS model.

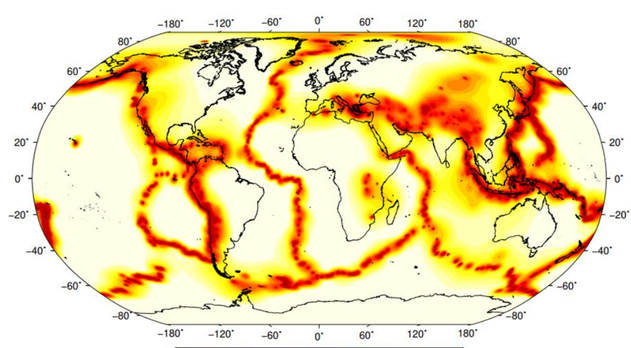

➢ Figure 5. Spatial variation of **background seismicity rates** (event/day/deg^2) for Mw>=5.15 calculated by Spherical spatiotemporal ETAS model.

Area	ν	A	α	c	p	D	q	γ	N	$\log L$
1	0.9050	0.2490	1.2778	0.0248	1.0865	0.5880×10^{-6}	2.1730	1.2017	20871	0.4009×10^{5}
2	0.9051	0.2489	1.2780	0.0248	1.0865	0.5880×10^{-6}	2.1725	1.2018	20871	0.4010×10^{5}
3	0.9052	0.2488	1.2781	0.0248	1.0866	0.5880×10^{-6}	2.1724	1.2019	20871	0.4010×10^{5}

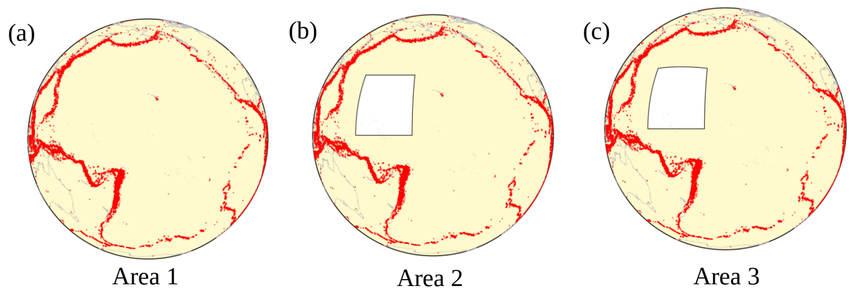

➢ Figure 6. An example of (a) Area 1, (b) Area 2, and (c) Area 3. The colored regions represent the study areas, and the red points represent earthquake locations.